TÜBİTAK

Turkish Journal of Earth Sciences

http://journals.tubitak.gov.tr/earth/

Research Article

Turkish J Earth Sci
(2017) 26: 57-72

doi:10.3906/yer-1610-10

# Marine effects on vertical electrical soundings along shorelines

**Emin Uğur ULUGERGERLİ***
Department Of Geophysics Engineering, Faculty of Engineering, Çanakkale Onsekiz Mart University, Çanakkale, Turkey

**Received:** 17.10.2016 • **Accepted/Published Online:** 17.11.2016 • **Final Version:** 13.01.2017

**Abstract:** Onshore applications of direct current resistivity (DCR) along shorelines suffer a short-circuit-like phenomenon due to electrical current flowing through a more conductive body of water rather than ground. Our study of the numerical simulation of DCR data with a three-dimensional forward model demonstrated that the apparent resistivity was reduced as a function of the sea depth and the distance of measurement site to the shoreline. Furthermore, it was concluded that the "marine effects" on DCR data (i.e. reduction in apparent resistivity) become nonnegligible as the ratio of half-electrode expansion (AB/2) to the distance to the shoreline is larger than one. The reduction in apparent resistivity reaches its highest levels as the ratio approaches ten. Our survey conducted along the coastal line of Northwest Turkey clearly showed that if the "marine effects" are left untreated, one- or two-dimensional inversion yields incorrect resistivities for underlying units and therefore undermines the credibility of survey results. In the paper suggestions are made to handle such situations.

**Key words:** Onshore, direct current resistivity, DCR, 2.5D inversion, electrical sounding, marine effects

## 1. Introduction

Onshore survey areas are subject to various geophysical studies. Electric and electromagnetic (EM) methods are common and are usually employed to delineate saline and freshwater boundaries. Fretwell and Stewart (1981) reported that Swartz (1937, 1939) was the pioneer in groundwater exploration and he used the direct current resistivity (DCR) method to locate freshwater lenses in salt-water bodies on the Hawaiian Islands. The main objectives of such research are to explore geology and to recover hydrogeological parameters. However, the possible influence of a low resistive (saline) body of water in the proximity of a survey area requires special treatment. Parameters such as frequencies of EM surveys, the distances to the coasts, bathymetries of the sea/lake floors, and the resistivity distributions of the land are the major elements of such influence (Santos et al., 2006). Similar to EM methods, DCR also suffers from the marine effect due to electrical current passing through more conductive body of water rather than flowing through the ground when a survey is conducted along a shoreline. This problem has not been addressed sufficiently in the literature; therefore, this manuscript focuses on the influence of a conductive body of water on DCR data recorded along a shoreline using representative geo-electrical models.

As computer science and hardware technology progress, tomography techniques have become a tool of choice in geophysical explorations (e.g., Loke and Barker, 1996; Sheehan et al., 2005). Multi-electrode systems gather large amounts of DCR data in reasonable times. Good coverage of the DCR tomography data leads to interpretations to obtain high resolution information for shallow zones while the deeper depths are still subject to conventional DCR surveys (e.g., Özurlan et al., 2006).

The DCR data are acquired by injecting current and recording voltage potentials over the ground surface where beneath lies a geological body of interest. It is a common convention to present the DCR data as apparent resistivities of the subject formation(s). These sets of apparent resistivities are translated into images of formations with true resistivities by minimizing the differences between model-generated data against observed ones by means of inversion. Although one-dimensional (1D) inversion of DCR data is still largely used, two-dimensional (2D) inversion is now replacing the 1D approach even in deeper targets. Presently, 3D DCR data have also become frequently available. However, the requirement of large AB expansions in perpendicular directions for monitoring the directional current flow makes 3D applications of DCR problematic for deep targets. As a result, shoreline DCR surveys lack sufficient expansion space to set up a station expanding perpendicular to the 2D profile due to physical constrains on the sea side. Asymmetric expansion (i.e. three-electrode configuration) was not considered for this study due to local conditions.

* Correspondence: emin@comu.edu.tr

The aforementioned difficulties in gathering 3D data and their limited penetration led us to use a 2D data set with 2D inversion as the main tool of interpretation for this study. It should be noted that if all stations are taken along a profile in line with each other and spatially dense enough, then 2D inversion can efficiently and accurately recover major geo-electrical structures beneath the profile. It is also possible to run a 3D inversion with 2D profiles but the result does not provide additional information between the profiles due to lack of data for cross-line profiles.

A DCR survey was conducted along the Aegean Sea coastline of Northwest Turkey to study the "short-circuiting effect" by a body of seawater on DCR data. The area is in the vicinity of Ezine, Çanakkale (Figure 1). The DCR data were acquired along the four parallel profiles with increasing distances to the coastline.

A preliminary 3D modeling study with a simplified geo-electric model of the area provided some information on the influence of the sea on the DCR curves. Follow-up 2D inversion of the DCR data revealed that the conductive seawater affected the magnitude of the apparent resistivity values, which, in turn, resulted in 2D inversion recovering a basement unit with lower resistivity than expected.

In the following sections, definitions, a summary of the local geology, and the survey parameters are given, respectively. Then a 3D forward calculation is used with a simplified test model to reveal the possible marine effect. 2D inversion of the acquired DCR data and comparison of its results with the forward model of the subject geo-electric model are presented with conclusions regarding the marine effects (short-circuiting) in DCR surveys adjacent to a body of water.

## 2. Definitions

We have used a configuration with a four-electrode system in our study. A and B represented current electrodes while M and N were the potential electrodes. The configuration parameters referred to the initial and end expansions of both current electrodes (AB) and potential electrodes (MN), while survey parameters were the station intervals and number of the stations along the profile. Each set of data gathered at the same station is called DCR sounding.

In terms of modeling, when the 3D distribution of current (point source) is considered over a 2D electrical model, the modeling scheme is usually called 2.5D (e.g., Xu, et al., 2000). The data can be acquired along a profile that crosses the targeted 2D geological structure perpendicularly. The only restriction required is the direction of the expansions at each station should be in line with each other and with the profile line. This is the case for all profiles and station data presented in this paper and 2D will refer to 2.5D modeling hereafter.

## 3. Geological setting and the data

The study area is located at the western end of the Biga Peninsula, NW Anatolia. Paleozoic metamorphic schists form the basement of the study area. Granodioritic intrusions occur in the basement. Rocks, andesite,

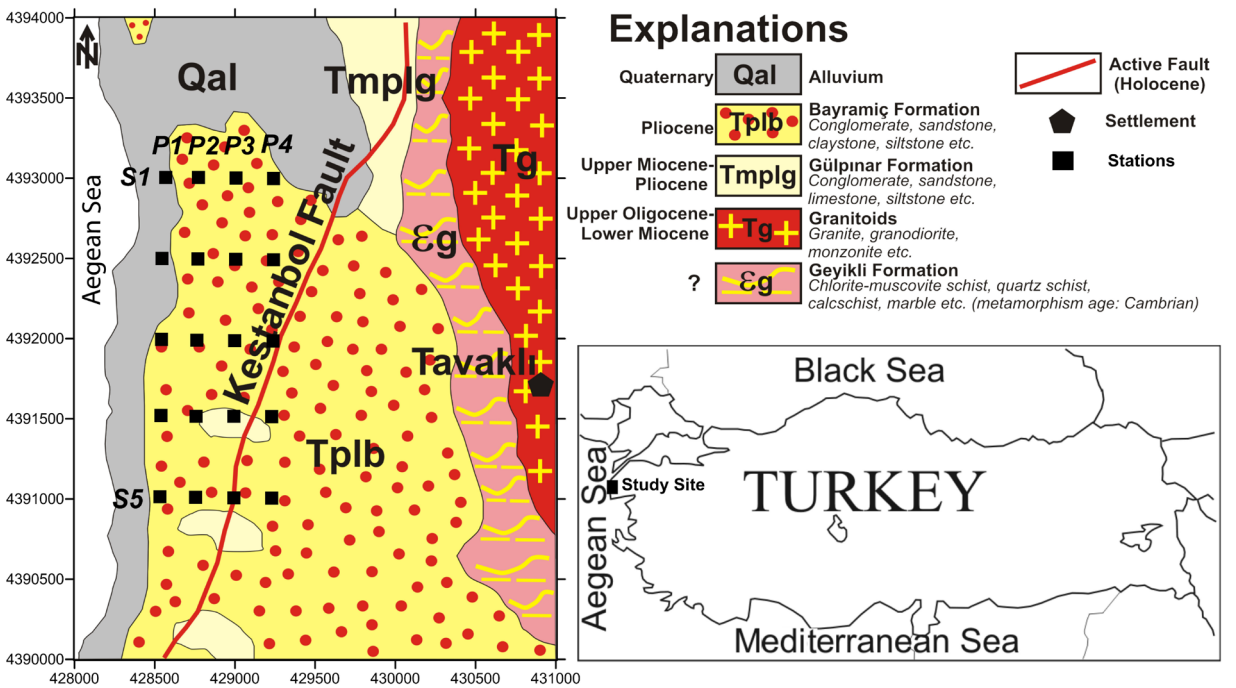


**Figure 1.** Study area. Black squares are the location of the stations. S1–S5 are stations while P1–P4 are profiles.

trachyiandesite granite, syenite, and quartzite, from the upper Permian overlay the basement. Neogenic limestone, sand, and marl make up the next unit in the stratigraphic sequence. The youngest ones are Quaternary alluvial units that cover the Aegean Sea coastline and are represented by sand/clay/gravel and blocks. The region has high geothermal energy potential and has been subject to various studies (e.g., Çaglar and Demirorer, 1999; Baba and Armannsson, 2006). The fracture zones with hot water circulations are the main targets for explorations.

Following the geo-electric models of Çaglar and Demirorer (1999), the summary of the sequences indicates that a conductive unit (alluvial) lies over the resistive unit (limestone, andesite family, and metamorphic units). In the case of sea intrusion into a shallow alluvial unit, fluid content and permeability control DCR response and, as a result, a conductive layer-like structure appears in the geo-electrical model. The resistivity of this layer can go as low as 1 ohm.m or less. On the other hand, both seawater intrusion and/or hot water circulations in deeper geological units usually occur through a fractured zone; then a conductive 2D feature (usually related to fault zones) appears in the geo-electric sections. Thus, geothermal exploration studies usually target these conductive fault zones in this region.

The data for this study were acquired along four profiles, all of which stretched as parallel as possible to the coastal line. The profile interval was 250 m and the first and the last lines were approximately 250 m and 1000 m away from the coastal line, respectively (Figure 1). Each profile had five stations at intervals of 500 m. All stations used the aforementioned configuration, and the current electrode expansions started from AB = 20 m and extended to AB = 4000 m with 22 logarithmically spaced intervals. In addition to the AB electrode expansions, the potential electrode interval, MN, was also increased after every three AB expansions with two overlapping readings. The ratio between AB/MN varied between 4 and 20. All nine segments of apparent resistivity curves, which occurred because of different MN interval settings, were shifted into agreement with the first one. Note that the shifting process was equivalent to using the first MN (2 m) value for all AB expansions. No other additional editing or conditioning was applied to the data.

**4. 3D Numerical approach**

Analysis of the off-profile effects was the subject of one of the earliest scientific discussions in the geophysics literature (Maeda, 1954a, 1954b; Van Nostrand and Cook, 1954). Authors both reported earlier studies and discussed possible analytic solutions for apparent resistivity over dipping beds. Telford et al. (1990) showed how the dipping bed or vertical contact leads to errors in estimating both depth and resistivity. Later Georgescu et al. (2010) revisited the problem. Besides the analytical solution, Queralt et al. (1991) tackled the problem numerically and presented an algorithm for 2D electrical resistivity modelling using the finite element method. They also provided a solution to the transformed potential of a point source when computing response parallel to the strike direction over a layered earth terminated by a cliff. In either case, off-profile structures (opposite side of the strike) were assumed either a homogeneous unit or a layered-earth model or a perfect conductor or a perfect insulator (cliff). To reveal the sea influence on the DCR data acquired along the coastal line, a 3D numerical study was performed. A similar approach was employed to reveal saline water intrusion from a channel by Kruse et al. (1999). Despite the fact that countless combinations of survey parameters and geo-electric conditions existed, four key points of the simplified case were considered here: the variation in apparent resistivities with increasing distance to the coastline (D), increasing thickness of the sea layer (T), gradually dipping sea layer, and cliff effect. All conditions required calculation of the influence of off-profile features. A simple but representative 3D geo-electric model was built by setting up a 100-m conductive (10 ohm.m) unit representing the top alluvial cover sitting over a resistive basement (500 ohm.m), which depicted the regional metamorphic complex. The Aegean Sea was represented by an extremely conductive (0.3 ohm.m) unit (Figure 2).

Using the 3D forward code of Ersoy (2008), based on Dey and Morrison's (1979a) formula, the apparent resistivities were calculated for ten distances of D varying from 100 to 6000 m while T was fixed at 100 m (Figure 3).

With this setting, the influence of the conductive sea unit appeared on the apparent resistivity curve as if it were a fictitious conductive layer between the two distinct resistive units. In Figure 3, the effect of the fictitious conductive layer appears as through between AB / 2 = 300 and 2000 m in line with the square marker (D = 100), then shifts towards larger AB/2, and becomes negligible when D approaches the exploration range of the maximum electrode expansion (~AB/3 > 6000), rendering it equivalent to the response of a two-layered model. As a result, the curves respond to the conductive sea unit at different AB expansion as function of D.

This information can help us to separate the effects of off-profile structures from the features that lie below the profiles and can be used later for conditioning. The second consideration was the effect of the thickness of the sea layer, T. In this case, T was increased gradually from 20 to 5000 m while D was fixed at 150 m (Figure 4). D was selected large enough so that the effect of the basement appeared in the curve before the effect of the conductive sea unit dominated

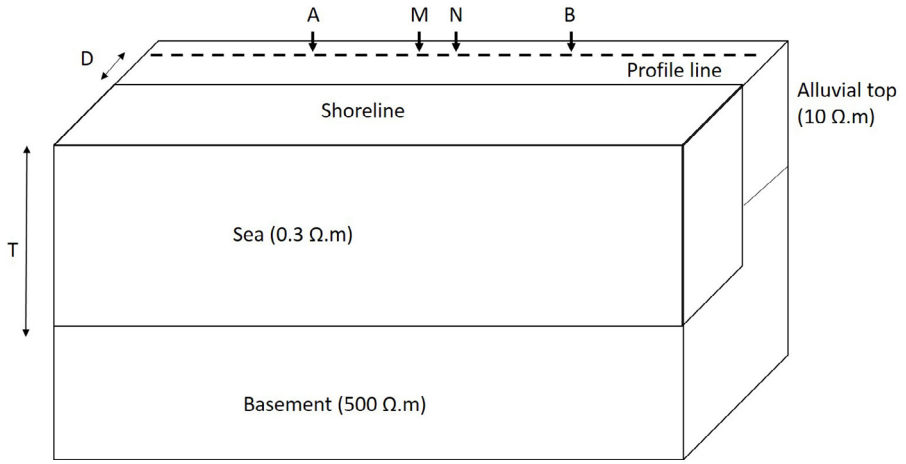


**Figure 2.** Conceptual 3D model for the study area. The sedimentary unit is 10 ohm.m, the basement is 500 ohm.m, and the sea is 0.3 ohm.m. The thickness of the sedimentary unit is 100 m. D is the distance to the coastline. T is the thickness of the sea layer.

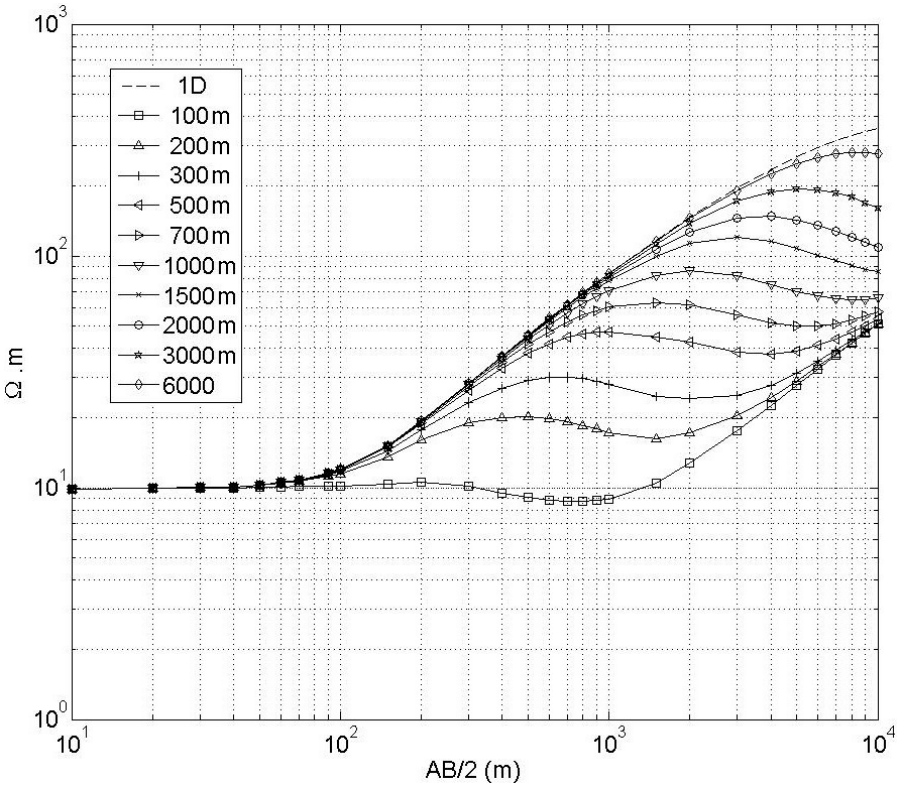


**Figure 3.** Apparent resistivity vs. AB/2 with increasing distance to the sea line (D (m)). The thickness of the sea layer (T) set to 100 m. The 1D curve is the response of a model without a sea unit.

the entire trend. If the T are smaller than maximum AB/2, the sea effect can appear as a conductive, mid-unit on the curve. If T is larger than maximum AB expansion, then the sea can appear as an artificial conductive basement and the effect of the resistive actual basement would vanish from the apparent-resistivity curve. As a result, if T is greater than D, the conductive unit can conveniently mask the resistive basement, which in turn will lead to erroneous evaluation of the model.

An interesting case occurred when T = 20 m. The amplitude of the apparent resistivity values related to the basement (AB/2 > ~ 1000 m) decreased to ~75% of its

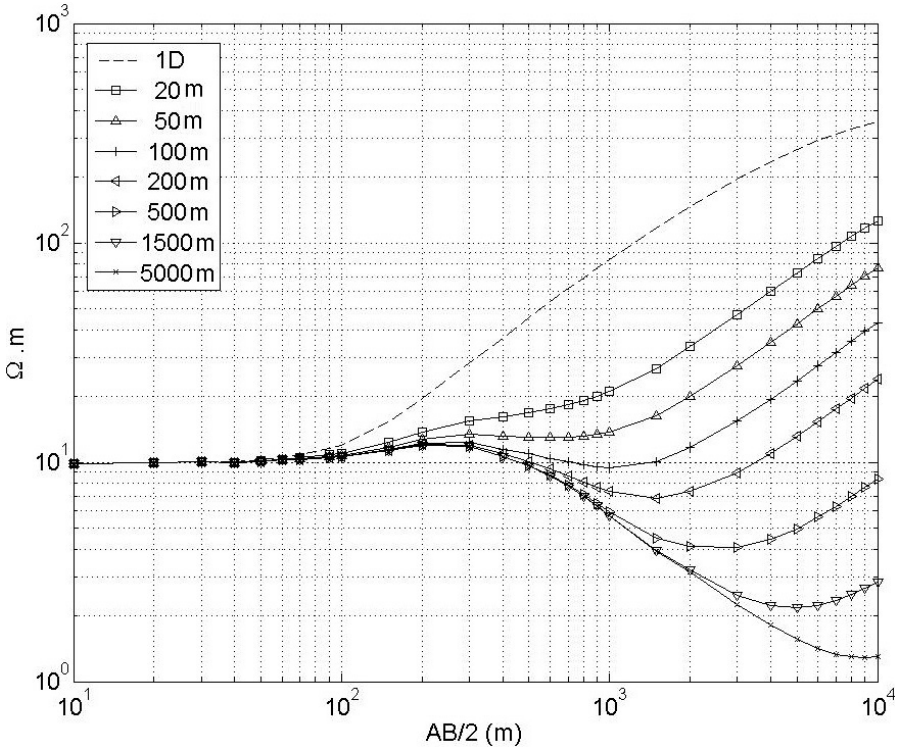


**Figure 4.** Apparent resistivity vs. AB/2 with increasing thickness of sea layer (T (m)). The distance to the coastline (D) set to 150 m. The 1D curve is the response of a model without a sea unit.

1D counterpart values obtained from a model without a sea unit. Considering realistic survey conditions, this reduction could easily prevent distinguishing the existence of any influence, and in turn leads to inversion to recover the basement unit with lower resistivity values than actual.

Apparent resistivities are functions of current flowing through the earth and the voltage drop between the potential electrodes. The path of the current defines the magnitude of the voltage drop. Simply, the more conductive the path is, the less the voltage drop is. The ratio of apparent resistivities over the different geo-electric conditions is equivalent to the rate of the voltage drop for fixed current injection. Therefore, the ratio between two apparent resistivity curves can be taken as an indicator for the contribution of geo-electrical structures to apparent resistivities.

$$\text{ratio} = \frac{\rho_a - \rho_{as}}{\rho_a} \qquad 1$$

where $\rho_a$ is apparent resistivities when D is infinite, equivalently the 1D case, and $\rho_{as}$ is the curve when D is finite. The sample curves are presented in Figure 5. Figure 5 also presents the ratio for increasing D vs. rD, where AB/2 normalized with D, that is rD = (AB/2)/D.

When AB/2 exceeds 100 m (rD = 0.5) the apparent resistivity curves present some deviations (see Figure 3). The bigger the rD is, the higher the deviation is. The amount of deviation is related to the path of the current flow. The ratio in Figure 5 indicates that more than 80% of the current flows through the sea at larger rD (>10). Figure 6 presents ratio for increasing T vs. rT, where AB/2 normalized with T, that is rT = (AB/2)/T.

T has also influence on the data (Figure 6). However, the relation is very complex due to D, which also affects the ratio. The rT curve for T = 20 m (square marker in Figure 6) indicates that the maximum effect occurs when rT ~ 75, that is, the shorter expansions are relatively safe from marine influence. If T increases, the rT value for the maximum effect decreases, which shows that downward deviation will increase on the curve. The AB values, apparent resistivities of which are deviated, will still be related to D.

The third consideration was the effect of the gradual dipping of the sea layer. In this case, the marine bathymetry had gradients of approximately 10%, 30%, and 60% while the D was fixed at 100 m. For low dipping gradient, the sea effect can appear as a conductive basement on the curve (Figure 7). If the gradient is very steep, approaching the vertical boundary, once again, the conductive unit can

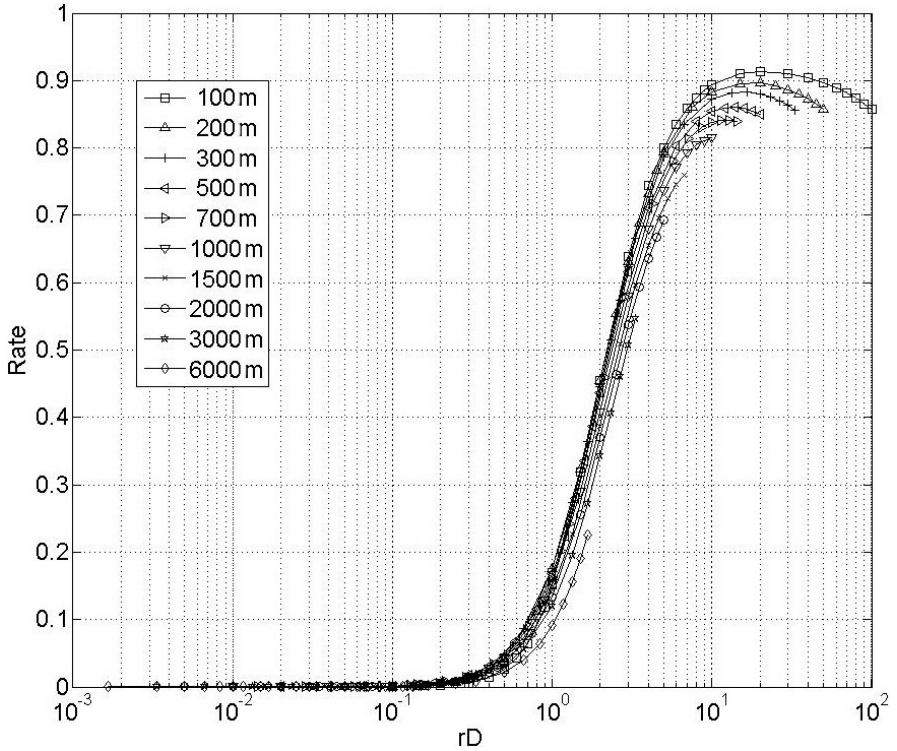


**Figure 5.** The ratio (Eq. 1) vs. normalized distance to the sea line (D (m)). Thickness of the sea layer (T) set to 100 m.

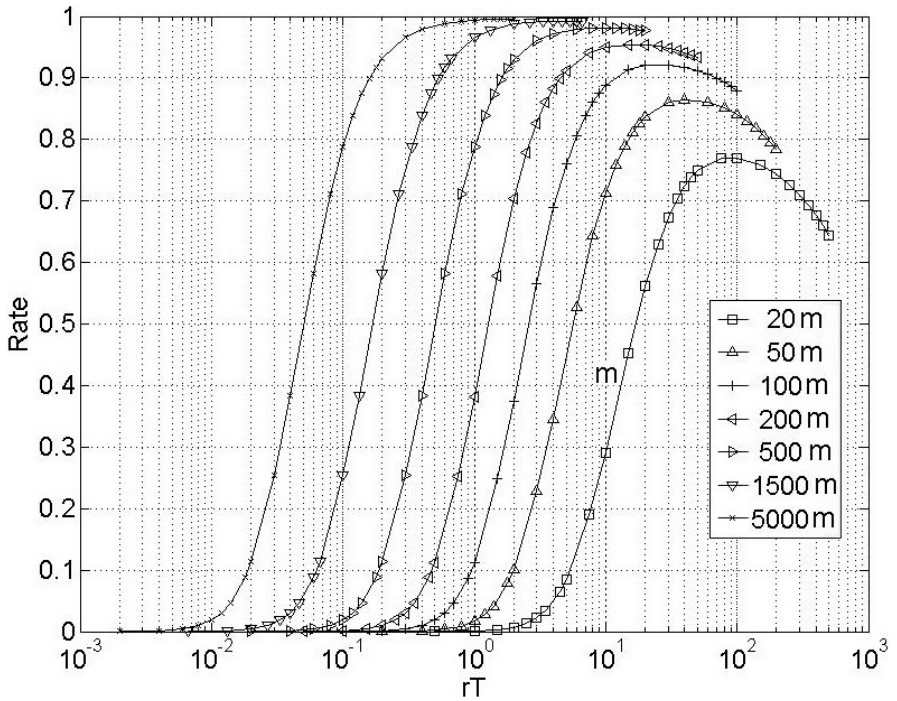


**Figure 6.** The ratio (Eq. 1) vs. normalized thickness of the sea layer (T(m)). The distance to the sea line (D) set to 150 m.

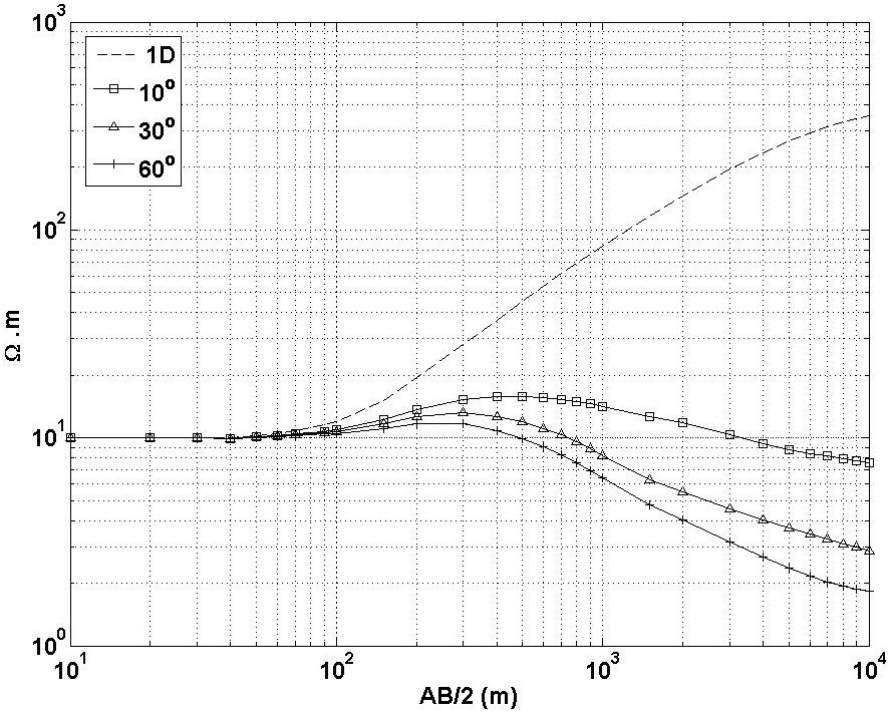


**Figure 7.** Apparent resistivity vs. AB/2 with gradually dipping sea layer. The distance to the sea line (D) set to 100 m. The 1D curve is the response of a model without a sea unit.

conveniently mask the resistive basement, which in turn will lead to erroneous evaluation of the model.

The fourth consideration was the effect of the cliff at the shoreline. In this case, both T and D are fixed at 100 m while cliff height (H) varies from 2 to 1000 m. The reference model represents a top alluvial cover sitting over a resistive basement without any conductive sea unit.

The effect of the cliff and conductive sea body presents a combination of influences of T and D given in Figures 3 and 4 (Figure 8). Figure 9 presents the ratio for increasing H vs. rH, where AB/2 normalized with H, T, and D, that is rH = (AB/2)/(H × T × D). Due to the selection of D and T, when H is smaller than 100 m the conductive sea body dominates curves through between AB/2 > 100 and 2000 m (Figure 8). When H exceeded 100 m, the influence of insulator appeared on the apparent resistivity curve as if it were a fictitious resistive layer overlaying a conductive one. In other words, the apparent resistivity curves present a four-layered earth model instead of a two-layered model.

This result also appears in Figure 9; the sign change (rH > 2e-3) indicates that the source of influence switches from conductive sea body to insulator facing cliff, that is, the influence of a low cliff will be masked by a fictitious low resistive layer whereas the influence of a high cliff will replace the fictitious conductive layer only if T is smaller than H.

**5. Computational tools and methodology for processing**

Various research papers on 2D inversion of DCR data and modeling for similar conditions as in this study can be found in the literature. Rijo et al. (1977) and Pelton et al. (1978) used the finite element code of Rijo (1977) for forward solution and inverted DCR and induction polarization data, respectively. Uchida and Murakami (1990) and Uchida (1991) presented a FORTRAN code for 2D interpretation of resistivity sounding data. The forward routines mentioned above are commonly based on the finite element method (FEM, e.g., Rijo, 1977; Uchida, 1991) or finite differences method (FDM, e.g., Dey and Morrison, 1979b).

We have developed a 2D inversion code for DCR soundings by combining the solution of Poisson's equation via FDM yielding a forward solution and damped least square method for inversion. Dey and Morrison (1979b) give the details of the finite differences equations for area – discretization over the mesh that we used below each sounding. Because we are dealing with independent electrical soundings, two meshes are needed, namely a model mesh and a calculation mesh. For the model mesh, we used the input data and survey parameters for constructing the desired (or initial) geo-electrical model. The calculation mesh was the actual one used in FDM for forward calculations.

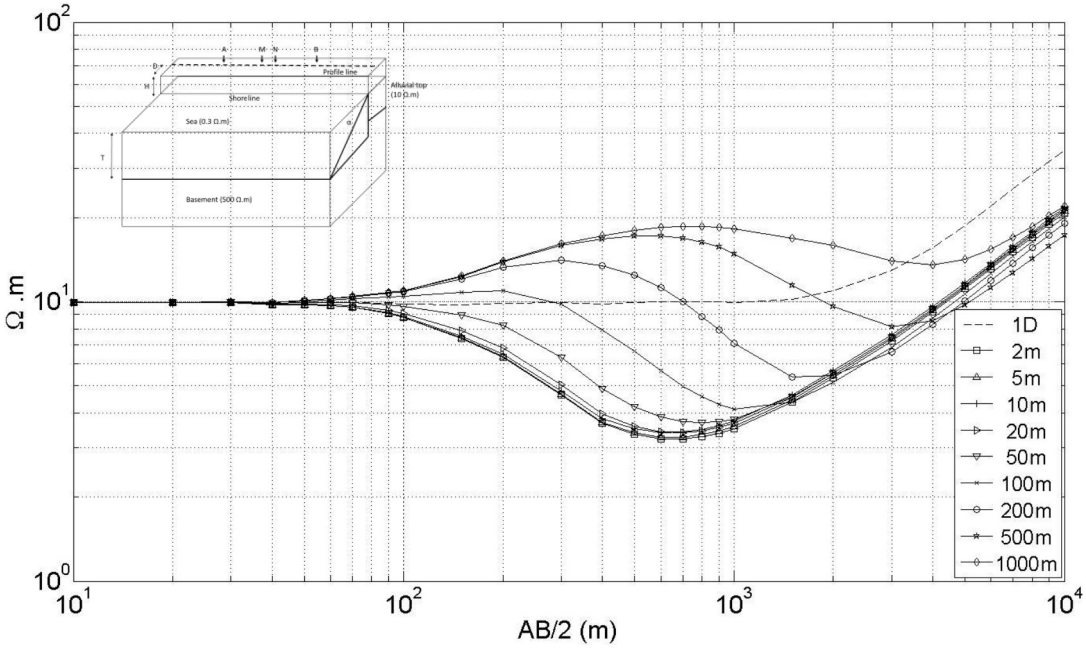


**Figure 8.** Apparent resistivity vs. AB/2 with increasing cliff height (H(m)). Both thickness of the sea layer (T) and distance to the sea line (D) set to 100 m. The 1D curve is the response of a model without a sea unit.

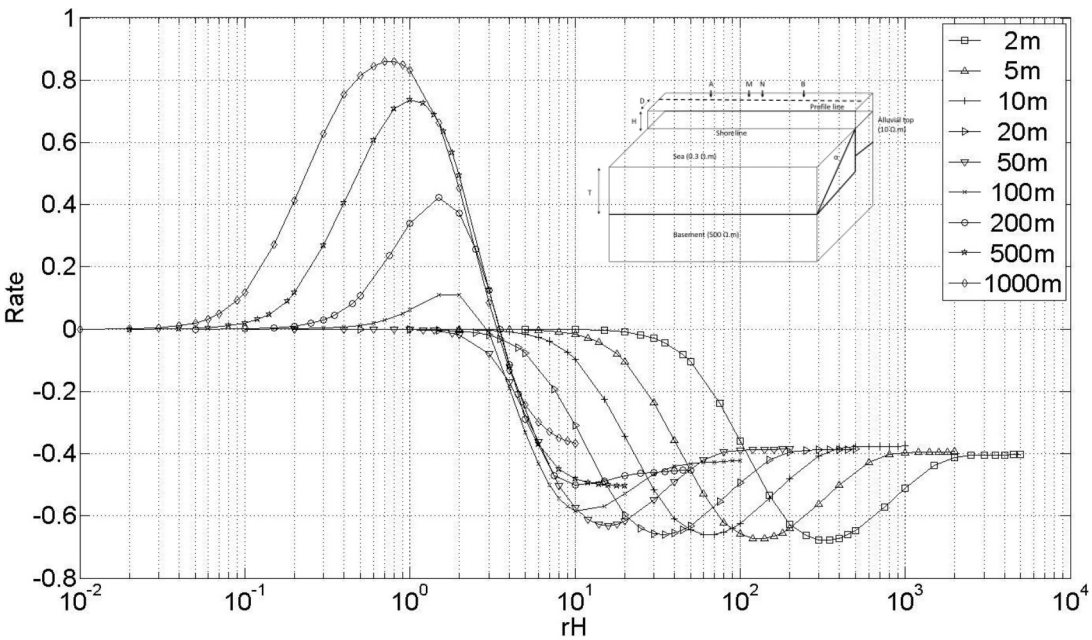


**Figure 9.** The ratio (Eq. 1) vs. normalized distance to H(m), D, and T. Thickness of the sea layer (T) and distance to the sea line (D) set to 100 m.

A predefined calculation mesh was used for all stations. It has 112 and 67 cells in the x and z directions, respectively. Expansion of the cell width in the x and z directions is in accord with the survey parameters. On the other hand, the model mesh for the profiles consists of 32 and 60 cells in the x and z directions, respectively. Five cells with variable width are placed between the stations. The depth of boundary of the last cell is extended up to 12,000 m.

The conductivity of each block (σ) of the model mesh is used as a parameter in the inversion stage, and then the result of 2D inversion is presented on the same mesh. An

equation for a nonlinear and ill-posed inversion problem is given as (e.g., Menke, 1989; Meju, 1994) as follows:

$$\Delta P = (A^T A + \beta I)^{-1} A^T \Delta G \quad (2)$$

The definitions of the variables are given as follows: A is a matrix consisting of partial derivatives J and smoothing matrices C,

$$A = \begin{bmatrix} J \\ C \end{bmatrix} \quad (3)$$

where

$$C \cdot \Delta P = 0 \quad (4)$$

β is a damping factor and is calculated for each iteration via

$$\beta(j) = ((0.01 \times 7^j) \times 10^{(j-1)})/j; \; j = 1, 2, \ldots, 10, \quad (5)$$

where j is a counter for damping factors. Ten different values are used in each iteration. ΔG is a vector of logarithmic discrepancies between observed and calculated apparent resistivity augmented with zeroes. ΔP is a logarithmic update vector for initial model parameters, σ

$$^{k+1}\sigma_i = 10^{\log(^k\sigma_i) + b\,\Delta p_i} \quad (6)$$

where k and i are iteration and index for model parameters. Arbitrary constant b is set as 0.3.

The code stops with three criteria: the misfit reaches the preselected threshold value, the number of iterations reaches the preset value, or fractal variation in misfits between sequential iterations is less than 1e-3. Measure of misfit, e, is calculated as

$$e = \left( \left[ \log \rho_a^o - \log \rho_a^C \right]^T \left[ \log \rho_a^o - \log \rho_a^C \right] / N \right)^{1/2} \quad (7)$$

where $^o$ and $^c$ define observed and calculated apparent resistivities, respectively.

The threshold for misfit should be selected in accordance with error level in the observed data. If observation errors are not available, as in our case, then it is found via a trial-and-error procedure.

## 6. Data evaluation

Figure 10 compares the apparent resistivities according to their distance to the coastline. For instance, the northern-most stations from all profiles are presented in the top left panel of Figure 10. Apparent resistivities are plotted versus AB/2 (m). In general, apparent resistivity values fluctuate around an average value of 10 ohm.m. Neither of the curves falls below 1 ohm.m. This indicates that there is no saline water intrusion in the region at extreme level.

Considering the deeper part (larger AB expansions), the ends of the curves ascend after descending and present a trough-like shape (AB/2 ~ 300 ~ 750 m) and the minima of the troughs vary from station to station. Recalling Figure 3, the apparent resistivity curves have similar patterns with the test data. The Aegean Sea, which lies along the survey area, was the culprit regarding the similarity by acting as a conductor in our data acquisition. All curves are expected to reach the resistive basement of a metamorphic complex after AB/2 > 1000 m.

## 7. 2D Inversion results

The results of 2D inversion are given in Figure 11. The first and last stations of profiles were at 0 and 2000 m, respectively, along the profiles. Triangles in Figure 11 indicate the locations of the stations. Initial models were for a homogeneous half-space of 100 ohm.m and initial misfit for P1 to P4 was 0.071, 0.081, 0.093, and 0.07, respectively. The inversion process was performed with a maximum of 50 iterations and the threshold value for misfit set 1.E – 3 after the trial-and-error procedure. The process stopped before reaching the maximum iteration limit due to insignificant improvement between the successive inversion steps. The final models of P1 to P4 had misfit values of 0.0028, 0.0037, 0.0059, and 0.0034, respectively. Observed (marker) and calculated (solid) apparent resistivity curves are presented in Figure 12. The fit between the observed and calculated data are good enough to accept that the recovered models are sufficiently converged, justifying further evaluations. The general features of final geo-electrical models obtained from 2D inversion and proposed geological evaluations are as follows: the top unit (0–100 m) is an alluvial zone. Then a conductive (<15 ohm.m) fractured unit take places between 100 m and 400 m. The conductive unit sits over a metamorphic basement (>20 ohm.m). Note that profile distances to the coastal line (D) were large enough to assume that top units in the recovered geo-electric models were realistically representative. On the other hand, the recovered resistivities for the basement vary 20–50 ohm.m less than expected and cover the entire sections below ~400 m depth.

## 8. Study results and discussions

Previous studies of our survey area in the literature (e.g., Çaglar and Demirorer, 1999) indicate the presence of a crystalline basement that should command high resistivities. However, 2D inversion of the DCR data shows the contrary. Speculations of fractures in the area that are invaded by saline sea water lowering the apparent resistivity can support the low resistivity profiles obtained from the 2D inversion to a certain extent. The geological studies of

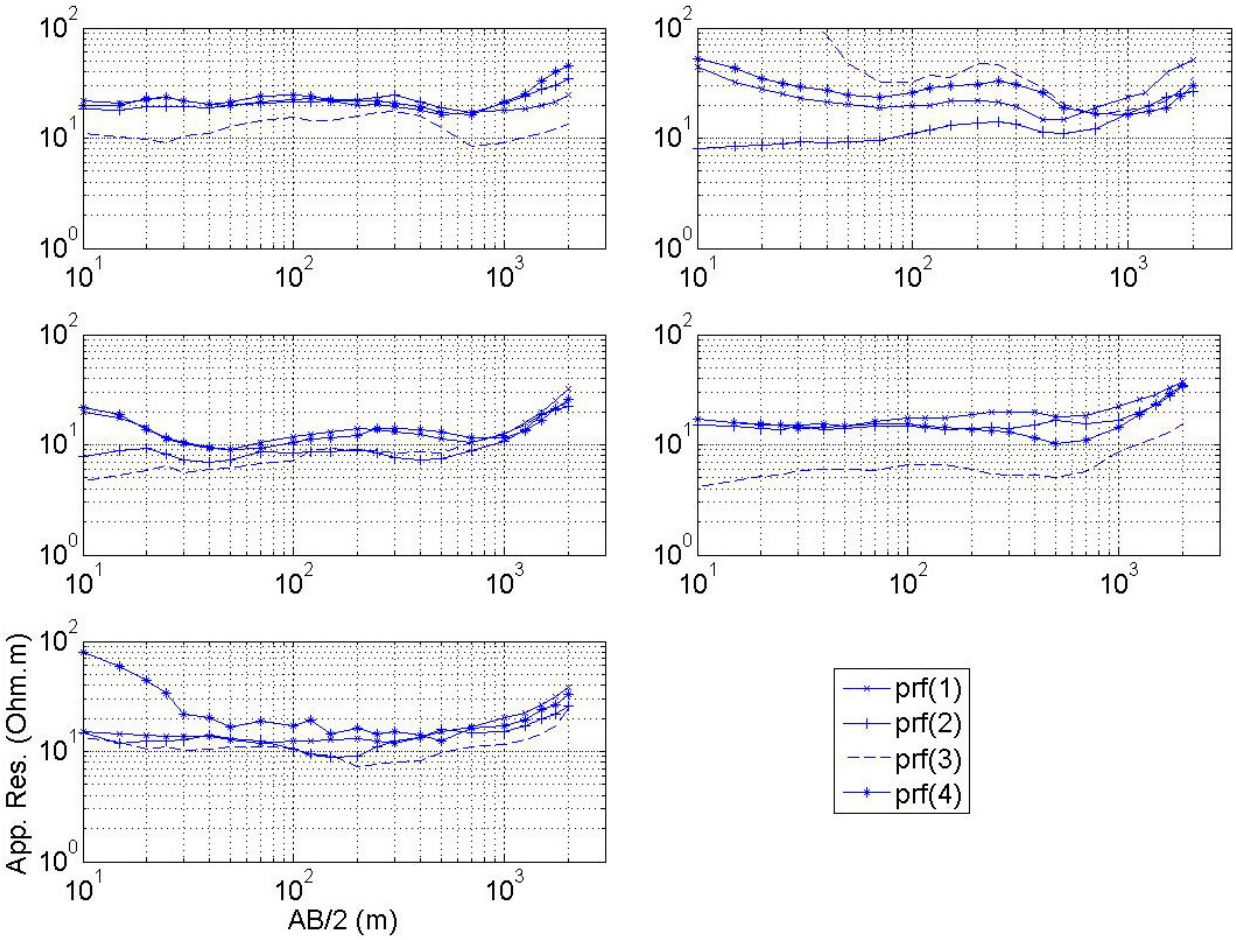


**Figure 10.** Stations from all profiles. First stations (top left), second stations (top right), third stations (middle left), fourth stations (middle right), last stations (bottom left). Vertical axes are apparent resistivity (ohm.m) while horizontal ones are half of the current electrode expansions, AB/2(m).

the area presents a local fault zone (Kestanbol fault in Figure 1) that may contribute to the lower resistivity values from uncompensated 2D inversion results. Nevertheless, the fault extends almost parallel to the survey line; hence, the current path would follow the fault zone and therefore ascending tails should not have appeared on the curves. None of our inverted models presented any overconductive (<1 ohm.m) unit that can be assigned directly to the body of seawater.

The contradictory results of geological findings against the DCR survey with 2D inversion and the ascending tails on the DCR curves led us study the "marine effects" on DCR data by 3D forward modeling. The study showed that all the field DCR data in this study were affected by the conductivity of the marine water. The 2D inversion routine underestimated the resistivity of the basement due to marine conductivity along the survey coastal line. The correct resistivity of the basement would have been much higher than the recovered resistivity from 2D inversion if there had been no sea in the vicinity of the survey area.

The effect of conductive sea body becomes complex if the basement is also conductive (not shown here). Considering the previous model (D = T = 100 m) with a resistive (100 ohm.m) cover unit sitting over a conductive basement (5 ohm.m), the deviation remains less than 5% for shorter (rd < 1.5) and larger (rD > 60) AB expansions. When AB/2 exceeds 500 m the apparent resistivity curves present deviations up to 50% but the influence of conductive sea diminishes for larger expansions (AB/2 > 3000 m). The affected range of AB expansions varies with the ratio of basement resistivities to sea resistivity. The larger the ratio is the wider the range becomes.

A 3D inversion program that could evaluate the contribution of structures residing along- and off-profile to survey data would be an appropriate way of overcoming such problem. The initial model should include both surface and sea-bottom topography and sea conductivity. Then the model recovered with 3D inversion would include better estimates for geo-electrical structures.

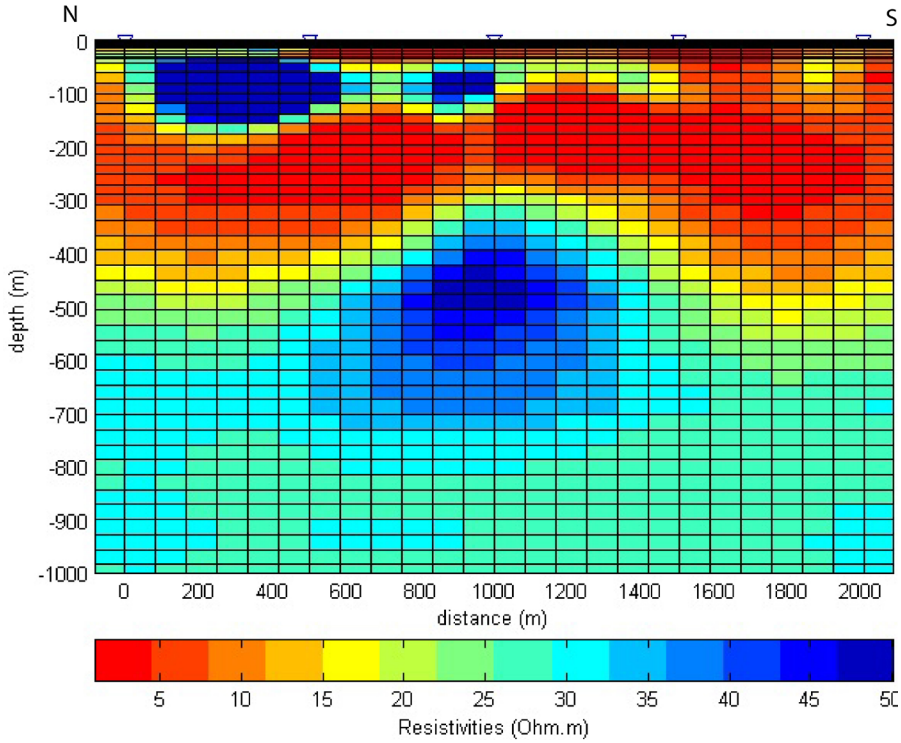


**Figure 11.** 2D models for each profile a) P1 b) P2, c) P3, and d) P4 defined in Figure 1. The first stations at 0 m at each profile.

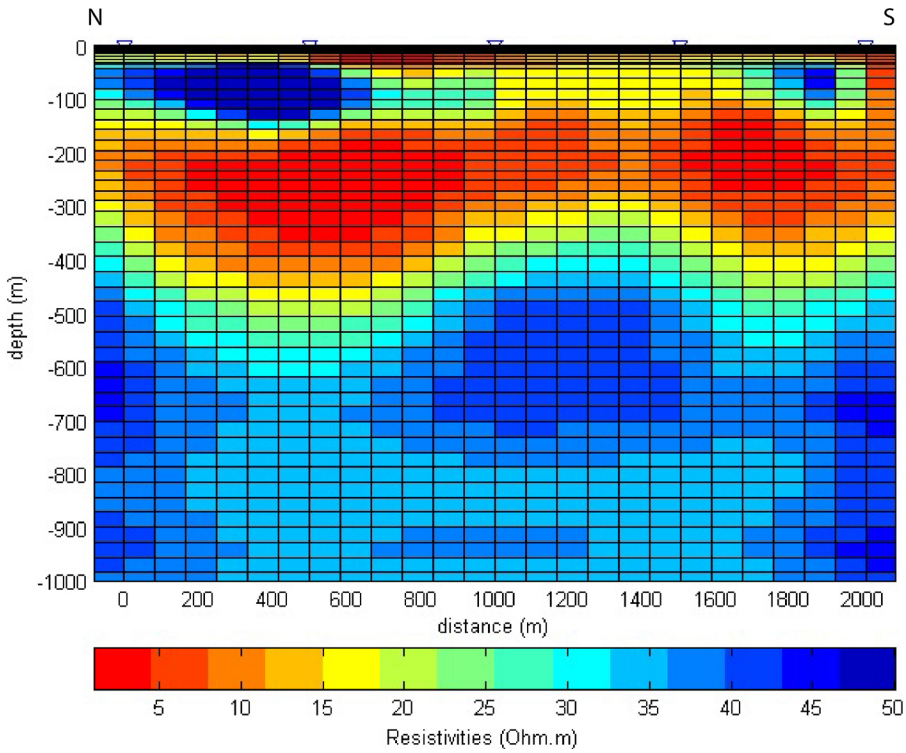


**Figure 11.** (Continued).

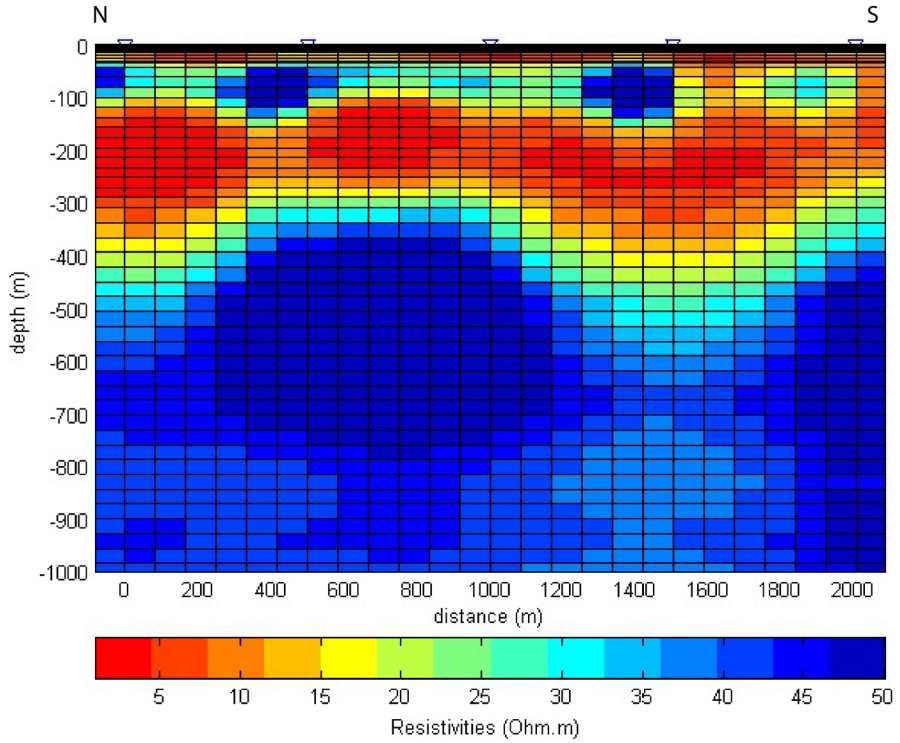


**Figure 11.** (Continued).

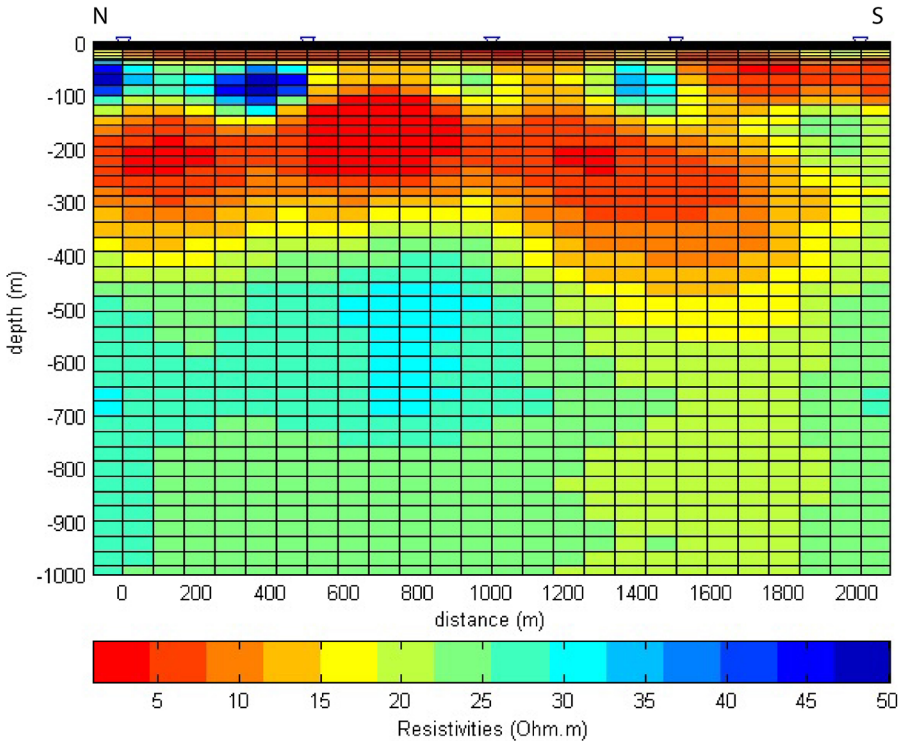


**Figure 11.** (Continued).

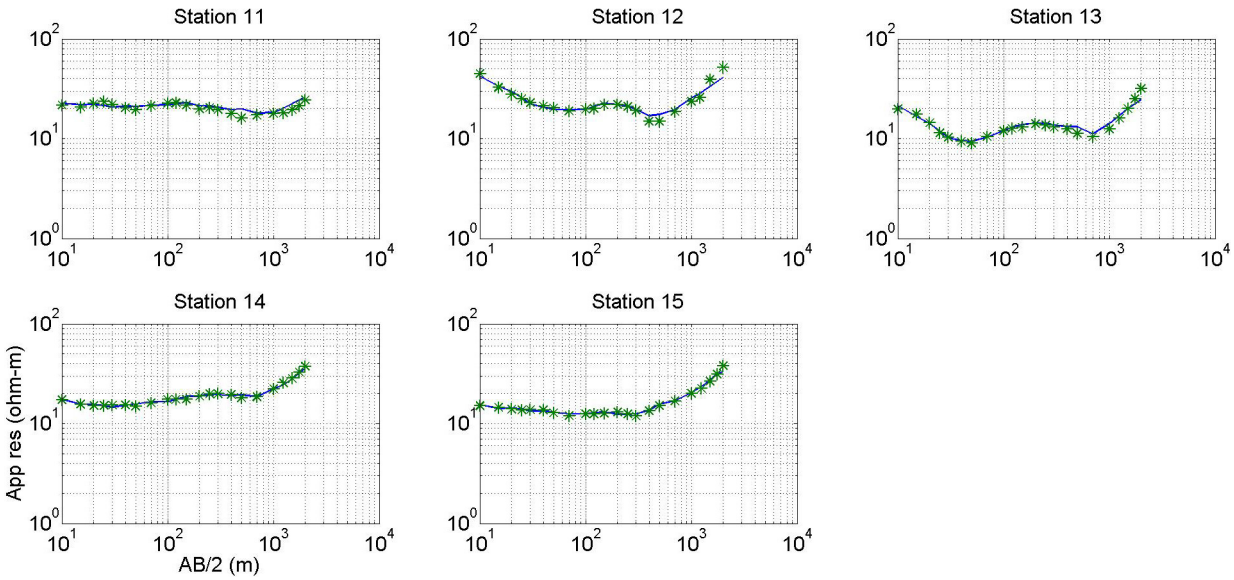


**Figure 12.** The apparent resistivity curves from inversion results. The markers are observed apparent resistivities and lines are calculated ones: a) Profile 1, b) Profile 2, c) Profile 3, and d) Profile 4.

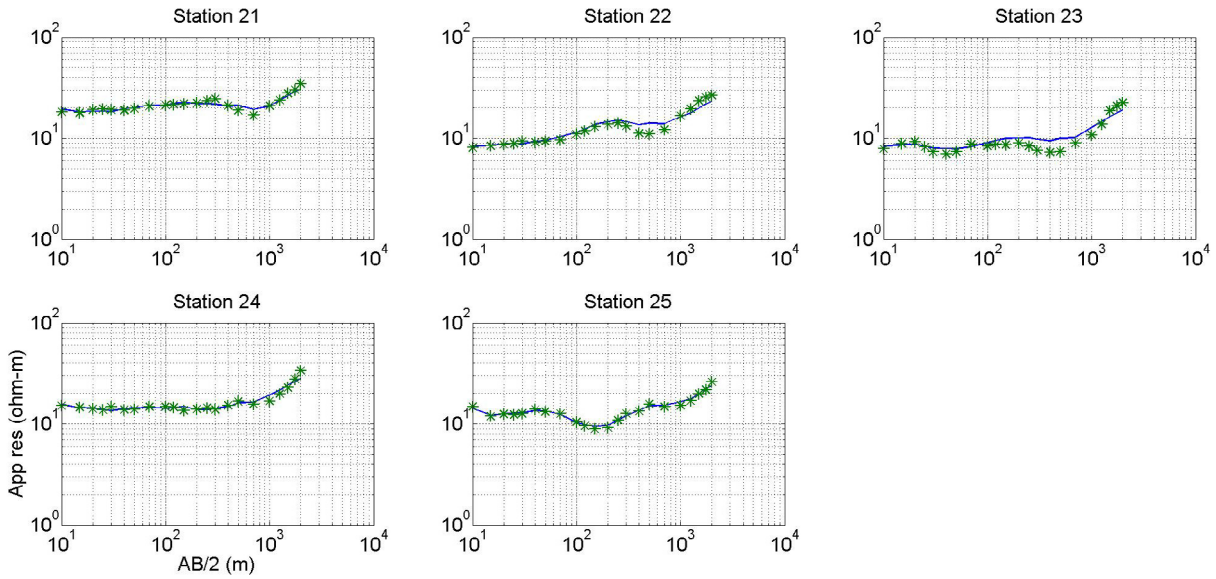


**Figure 12.** (Continued).

In the case of unavailability of the 3D inversion program, as shown in this manuscript, a 3D forward program and an approximate earth model provides information about the influence of a conductive sea body on survey data. Then the elaboration stage of the result of the 2D inversion program should take this information into consideration. A similar procedure was also suggested by Holcombe and Jiracek (1984), who recommended a procedure to recognize and decouple the effect of topography on resistivity data prior to 2D inversion.

The removal of the influence is not a linear problem to tackle. The form and magnitude of the influence are functions of the geo-electrical setting of the survey area. Removing the effect of conductive sea from observed data is equivalent to removing the contribution of one layer from the earth model and may be done by developing an iterative method following Basokur (1999). However, this approach is based on a 1D earth model and can also remove the signature of sought 2D structures from data set (Beard and Morgan, 1991; Basokur, 1999).

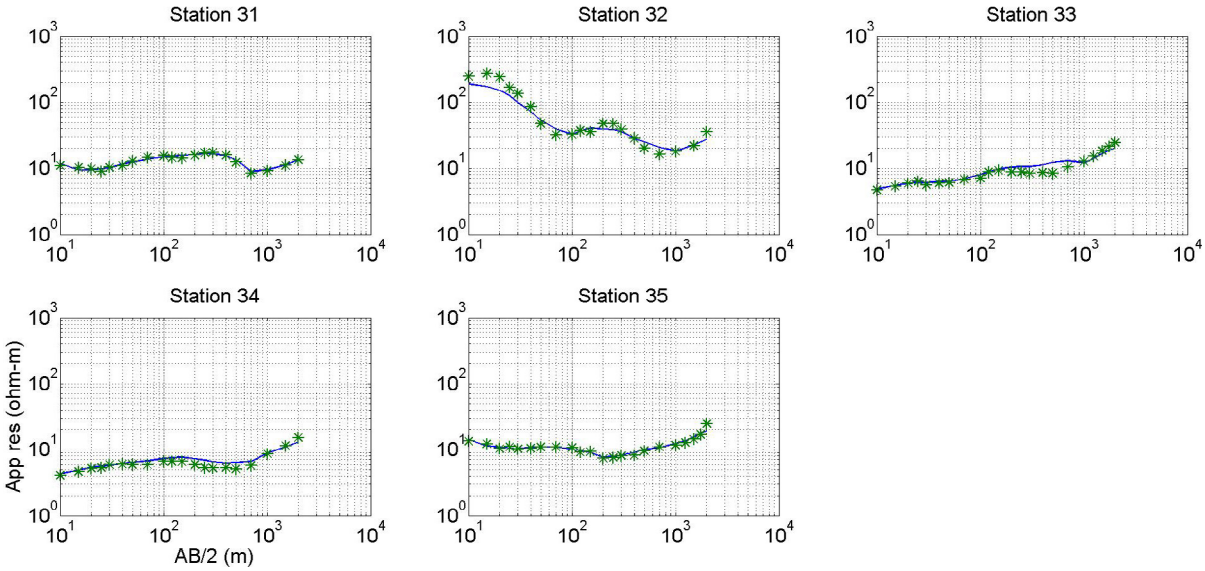


**Figure 12.** (Continued).

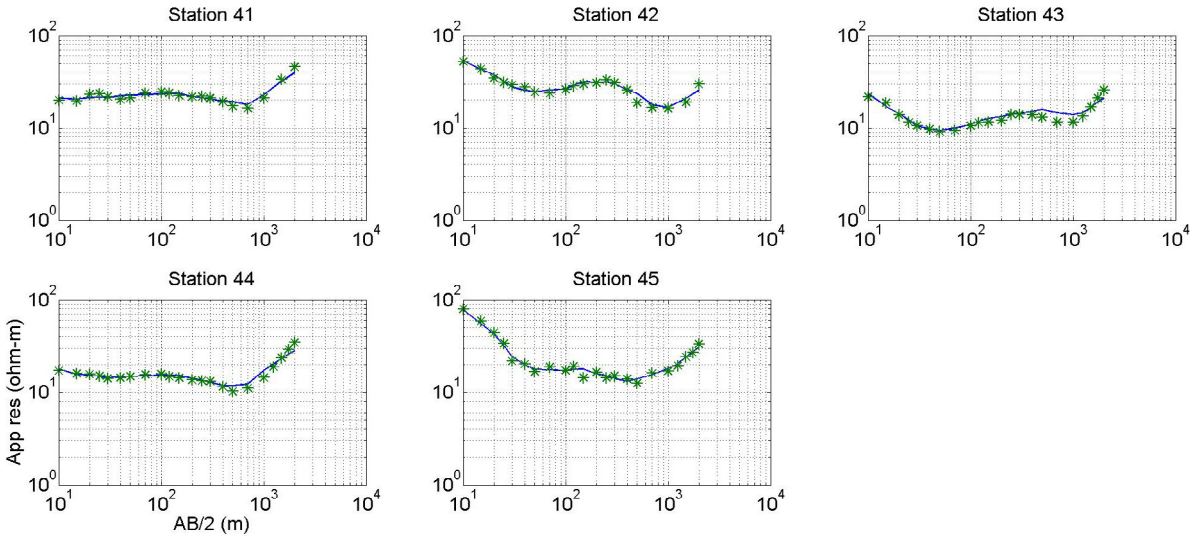


**Figure 12.** (Continued).

All findings are based on both a DCR survey and numerical studies. Therefore, the limitations and suggestions are valid only for the DCR method.

As an alternative approach, time domain EM (TDEM) either accompanies or replaces the DCR method for exploring deep targets. Toft (2001) and Holz et al. (2005) showed that a conductive fill-in (sea body in this study) has a serious effect on the TDEM data gathered nearby. The influence is significant as far as 300 m away from the coastal line regardless of sea bottom slope. If the model were deeper the effect would appear in much more distant locations. In the light of the findings presented in this paper, this may mean that the DCR method is much more affected by sea than for example central loop TDEM. However, additional numerical research is necessary to validate this comparison.

## 9. Conclusions

2D surveys will remain in demand in explorations because of the relative easiness of data gathering compared to 3D surveys. In addition, 2D schemes of DCR sounding methods are still applicable and efficient for surveys of geothermal or mining explorations. However, we recommend caution regarding the "marine effects" and topographic effect. Numerical simulations with simplified models and experience with field data resulted in the

following suggestions for handling such situations before 2D inversion:

1. Before the survey perform a 3D forward modeling study with local geomorphological and offshore conditions to check for the presence of such effects when surveys are along coastal lines of seas or lakes.

2. Refine survey parameters and, if possible, select or relocate survey sites.

3. After the survey, analyze data and mark affected expansions.

4. After 2D inversion, compare the recovered model with anticipated subsurface targets and, if there are any, delineate fictitious units with the help of step 3.

5. Evaluate results omitting fictitious units.

Additionally, our simulations showed that marine effect is a site-specific problem; therefore, practitioners should avoid arbitrarily applying any guidelines relating such effects to predefined geometry alone.

**Acknowledgments**

Thanks are due to H Çetin for providing the DCR data, B Ersoy for making her 3D code available, C Ertekin (MTA) for providing the geology map of the region, and M Yadegar for preparing figures. Thanks are extended to MM Altunbay for editing, clarifying, and fruitful discussions on the text and to one of the reviewers for reminding me of the effect of a cliff on DC sounding data.

## References

Baba A, Armannsson H, (2006). Environmental impact of the utilization of a geothermal area in Turkey. Energ Source 1: 267-278.

Basokur AT (1999). Automated 1D interpretation of resistivity soundings by simultaneous use of the direct and iterative methods. Geophys Prospect 47: 149-177.

Beard LP, Morgan FD (1991). Assessment of 2D resistivity structure using 1D inversion. Geophysics 56: 874-883.

Çaglar I, Demirörer M (1999). Geothermal exploration using geoelectric methods in Kestanbol, Turkey. Geothermics 28: 803-819.

Dey A, Morrison HF (1979a). Resistivity modeling for arbitrarily shaped three dimensional structures. Geophysics 44: 753-780.

Dey A, Morrison HF (1979b). Resistivity modeling for arbitrarily shaped two-dimensional. Geophys Prospect 27: 106-136.

Ersoy B (2008). Effect of shallow local structures on electrical soundings curves. Symposium On Geophysics And Remote Sensing In Determination Of Near-Surface Structures (article in Turkish with an abstract in English).

Fretwell JD, Stewart MT (1981). Resistivity study of a coastal karst terrain, Florida. Ground Water 19: 156-162.

Georgescu P, Ioane D, Niculescu BM, Chitea F (2010). Geoelectrical investigations of marine intrusions on the Romanian Black Sea shore. Geo-Eco-Marina 16: 85-92.

Holcombe HT, Jiracek GJ (1984). Three-dimensional terrain corrections in resistivity surveys. Geophysics 49: 439-452.

Hölz S, Hiller T, Burkhardt H (2005). Effects of dipping layers on TEM 1D-inversion. In: Ritter O, Brasse H (editors) 21. Kolloquium Elektromagnetische Tiefenforschung, pp. 197-206.

Kruse SE, Brudzinski MR, Geib TL (1999). Use of electrical and electromagnetic techniques to map seawater intrusion near the Cross-Florida Barge Canal. Environ Eng Geosci 4: 331-340.

Loke MH, Barker RD (1996). Rapid least-squares inversion of apparent resistivity pseudosections using a quasi-Newton method. Geophys Prospect 44: 131-152.

Maeda K (1955a). Apparent resistivity for dipping beds. Geophysics 10: 123-139.

Maeda K (1955b). Apparent resistivity for dipping beds- reply to preceding discussion. Geophysics 10: 144-147.

Meju MA (1994). Geophysical Data Analysis: Understanding Inverse Problem Theory and Practice: SEG Course Notes Series, 6, Tulsa: SEG.

Menke W (1989). Geophysical Data Analysis: Discrete Inverse Theory. New York, NY, USA: Academic Press.

Özürlan G, Candansayar ME, Şahin HM (2006). Deep resistivity structure of Dikili- Bergama region, West Anatolia, revealed by two dimensional inversion of vertical electrical sounding data. Geophys Prospect 54: 187-197.

Pelton HW, Rijo L, Swift CM Jr (1978). Inversion of two-dimensional resistivity and induced-polarization data. Geophysics 43: 788-803.

Queralt P, Pous J, Marcuello A (1991). 2-D resistivity modeling: an approach to arrays parallel to the strike direction. Geophysics 56: 941-950.

Rijo L (1977). Modeling of electric and electromagnetic data. PhD, University of Utah, Utah, USA.

Rijo L, Pelton WH, Feitosa EC, Ward SH (1977). Interpretation of apparent resistivity data from Apodi Valley, Rio Grande Do Norte, Brazil. Geophysics 42: 811-822.

Rücker C, Günther T, Spitzer K (2006). Three-dimensional modelling and inversion of dc resistivity data incorporating topography — I. Modelling. Geophys J Int 166: 495-505.

Santos FAM, Almeida EP, Gomes M, Pina A (2006). Hydrogeological investigation in Santiago Island (Cabo Verde) using magnetotellurics and VLF methods. J Afr Earth Sci 45: 421-430.

Sheehan JR, Doll WE, Mandell WA, Watson DB (2005). Detecting Cavities with Seismic Refraction Tomography: Can it be done? In: the Symposium on the Application of Geophysics to Engineering and Environmental Problems, pp. 989-1003.

Swartz JH (1937). Resistivity studies of some salt-water boundaries in the Hawaiian Islands. AGU Transac 18: 387.

Swartz JH (1939). Resistivity studies of some salt-water boundaries in the Hawaiian Islands Part II. AGU Transac 20: 292.

Telford WM, Geldart LP, Sheriff RE (editors) (1990). Applied Geophysics. Cambridge, UK: University Press.

Toft M (2001). Three-dimensional TEM modeling of nearsurface resistivity variations. MSc, University of Aarhus, Aarhus, Denmark.

Uchida T (1991). Two-dimensional resistivity inversion for Schlumberger sounding. Geophys Exp (Butsuri-Tansa) 44: 1-17.

Uchida T, Murakami Y (1990). Development of Fortran Code for the Two-Dimensional Schlumberger Inversion. Geological Survey of Japan Open-File Report, No. 150, 50p.

Van Nostrand RG, Cooks KL (1955). Apparent resistivity for dipping beds - a discussion. Geophysics 10: 140-144.

Xu S, Duan B, Zhang D (2000). Selection of the wavenumbers k using an optimization method for the inverse Fourier transform in 2.5D electrical modelling. Geophys Prospect 48: 789-796.